

## Anomaly Detection approach for the search of new resonances with fully-hadronic final state

A. CORVINO ON BEHALF OF THE ATLAS COLLABORATION

*INFN, Sezione di Napoli - Napoli, Italy*

*Dipartimento di Fisica, Università degli Studi di Napoli "Federico II" - Napoli, Italy*

**Summary.** — In recent years, the exploration of Beyond Standard Model phenomenology has become more and more important. One approach to handle this new hard challenge is to look at the data with minimum assumptions on the model, using Anomaly Detection (AD) techniques. Here, a novel application of AD is used to define a general signal region, where events are selected solely because of their incompatibility with a learned background-only model. Further, as an example of the possible approach of AD an application on a benchmark dataset of the unsupervised learning approach using Graph Neural Networks is presented.

### 1. – Anomaly Detection

The process under study is the production of a heavy-mass resonance  $Y$  decaying into an Higgs boson  $H$ , that decays into two bottom-quarks  $b\bar{b}$ , and a new resonance  $X$ . This channel has been chosen because of the strong coupling of the  $H$  boson with heavy particles, making the process as model-agnostic as possible. The only assumption on the  $X$  resonance is that its final state is fully hadronic. As no significant excess was observed, the results are presented as the upper limit on the production cross section of the process  $pp \rightarrow Y \rightarrow HX \rightarrow b\bar{b}q\bar{q}$  described in a general Heavy Vector Triplet model with two-prong signature, i.e. the  $H$  and  $X$  candidates can be reconstructed with only two jets.

**1.1. Event Selection.** – The mass of  $Y$  resonance is in the range  $[1.5, 6]$  TeV, while the  $X$  boson has a mass in the range  $[65, 3000]$  GeV [1].

The  $H$  and  $X$  bosons are produced with significant Lorentz boost due to the large mass of the  $Y$  resonance. It is possible to separate two regimes depending on the mass ratio between  $m_X$  and  $m_Y$ . If  $m_X/m_Y \leq 0.3$  the regime is called **merged** and the  $X$  boson is boosted and is reconstructed as a single large- $R$  jet - i.e. jets reconstructed with anti- $k_T$  algorithm with a  $R$  range parameter of 1.0. If the ratio is  $m_X/m_Y > 0.3$ , then the  $X$  boson can be reconstructed as two single small- $R$  jets, and this regime can be called as **resolved** [3].

This decay channel, whose Feynman diagram is represented in Figure 1 is pre-selected using the following conditions:

- The mass of either the leading or the sub-leading large- $R$ , ordered in  $p_T$ , is greater than 50 GeV;
- The leading large- $R$  jet  $p_T$  must be greater than 500 GeV;
- The invariant mass of the two leading large- $R$  jets must be greater than 1.3 TeV.

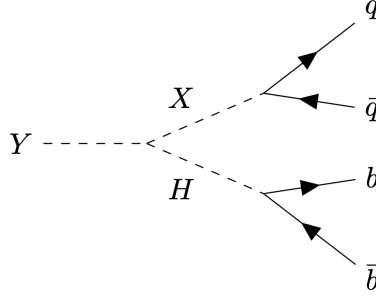


Fig. 1. – Feynman diagram for the fully hadronic decay used for this analysis.

Once the preselection is done, the next step has been the tagging of the  $H$  candidate among the large- $R$  jets. The channel  $H \rightarrow b\bar{b}$  has the highest branching ratio for the  $H$  decays, and a Machine Learning technique [2] is used to tag it. Once one of the jet is tagged as  $H$  candidate and the other one is tagged as  $X$  candidate and a selection is done on it.

**1.2.  $H$  and  $X$  candidate tagging.** – Boosted Higgs bosons decaying via the dominant decay channel  $H \rightarrow b\bar{b}$  are essential in several LHC searches. Usually, ATLAS identifies these  $H$  bosons by applying flavour-tagging algorithms on the constituents of large- $R$  jets, but it is possible to obtain a more accurate tagging using a feed-forward neural network and its outputs, that can describe the variable called  $D_{H_{bb}}$ .

In the two-prong events, both the large- $R$  jets of  $H$  and  $X$  candidates pass through the Neural Network and the jet with the highest  $D_{H_{bb}}$  output is selected as the  $H$  candidate. In addition, a calibrated cut-off in the  $D_{H_{bb}}$  distribution (Figure 2a) is used to decide if a jet can be tagged as  $H$  or not. Another condition used is on the mass of the jet: the  $H$  candidate mass must be in the range [75, 145] GeV. These two conditions define the **Signal Region** as shown in Figure 2b.

The  $X$  candidate is tagged in two different ways: as two-prong signal or as anomaly. A multivariate discriminant, called  $D_{Tracks}^2$ , is built to give as output the likelihood of the jet to be formed by two collimated small- $R$  jets. Lower  $D_{Tracks}^2$  correspond to a higher likelihood of the  $X$  candidate to be a large- $R$  jet. The merged region is thus defined with  $D_{Tracks}^2 < 1.2$  as shown in Figure 3a.

When the  $X$  substructure is formed by two non-collimated small- $R$  jets deriving from its decaying, then the  $X$  candidate lies in the resolved kinematic regime. This region is necessary to increase the sensitivity to signals in a wider phase space and is chosen to be orthogonal to the merged selection (i.e.  $D_{Tracks}^2 > 1.2$ ). Also, there are additional cuts on two more kinematic variables to discriminate signal and background:

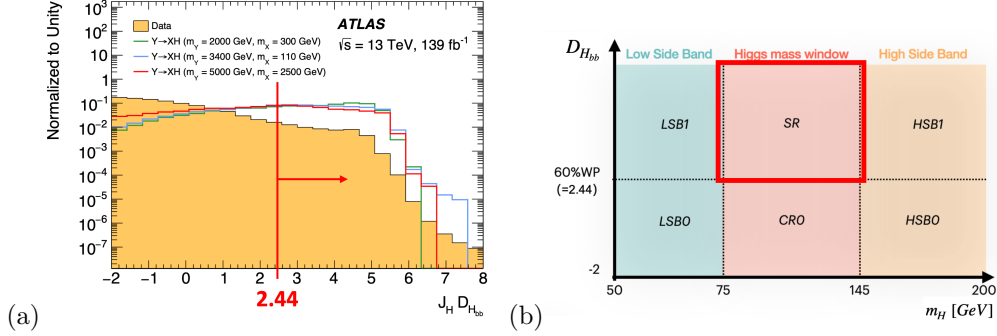


Fig. 2. – (a)  $D_{H_{bb}}$  distribution for data and for 3 different couple of  $m_X$  and  $m_Y$  MC simulations, with the cut-off at 2.44. (b) Phase space for the selection of  $H$  boson candidate using the mass of the candidate and the value of  $D_{H_{bb}}$ .

- $|\Delta y| < 2.5$  between the two small- $R$  jets;
- $p_{T_{bal}} < 0.8$  - where the  $p_T$  balance is defined as  $p_{T_{bal}} = \frac{p_{T_{J_1}} - p_{T_{J_2}}}{p_{T_{J_1}} + p_{T_{J_2}}}$

The final region is defined as Anomaly Region and is a discovery region based on a data-driven anomaly score (**AS**). This region is filled with events incompatible with SM events, treating them as signal candidates - Figure 3b. The AS is computed using a fully unsupervised Variational Recurrent Neural Network trained over jets with  $p_T > 1.2$  TeV and modelled as a sequence of constituents four-vectors. This is done to be sensitive to alternative  $X$  decay hypotheses other than two-prong - e.g. three prong, heavy flavour and dark jet. The AS region is defined with the flat cut  $AS > 0.5$ .

**1.3. Background Estimation.** – The background in the Signal Region arises from high  $p_T$  multijet events, and simulations for such processes are expensive to generate, so it is operated by a data-driven approach. Looking at Figure 2b, the shape of expected  $m_{JJ}$  distribution in the SR is obtained from data in CR0. Weights are derived that can be applied to HSB0 to reproduce the shape in HSB1. The validation of this procedure was done by applying the weights to data in LSb0 and comparing the resulting  $m_{JJ}$  spectrum to that observed in LSb1.

The re-weighting function is defined as the ratio of the multi-dimensional probability distribution functions of the data in HSB1 ( $pdf_1$ ) to data in HSB0 ( $pdf_0$ ):

$$w(x) = \frac{pdf_1(x)}{pdf_0(x)}$$

A Deep Neural Network learns  $w(x)$  in the training region HSB, then is validated in the validation region LSb and finally extrapolated in the Higgs mass window. The training is done before the  $D_{Tracks}^2$  and  $AS$  categorization and the DNN features used are: the  $H$  candidate 4-momenta, the number of tracks associated to  $H$  candidate and the 4-momenta of the leading and sub-leading small- $R$  jets associated with the  $H$  candidate.

**1.4. Results.** – The  $p$ -value threshold is set to  $p < 0.01$  in order to determine the incompatibility with background-only hypothesis. Across the  $m_X$  range,  $p$ -values show

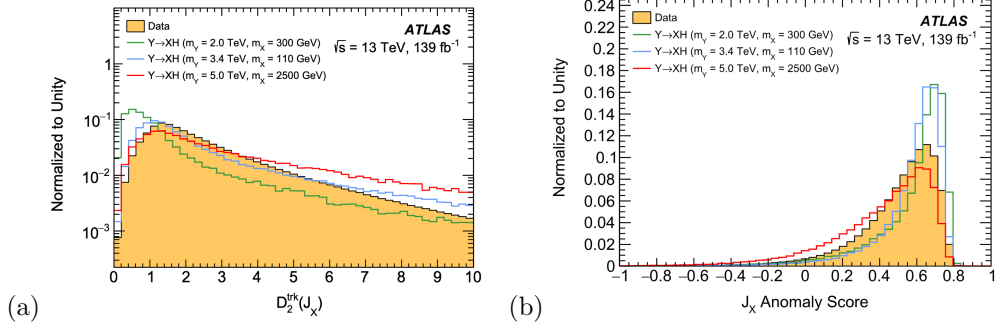


Fig. 3. – (a)  $D_2^{rk}$  distribution for data and for 3 different couple of  $m_X$  and  $m_Y$  MC simulations. This is one of the variable used for the classification in the two regimes for the  $X$  candidate in the two-prong region. (b) Distribution of AS in data and for 3 different couple of  $m_X$  and  $m_Y$  MC simulations.

good compatibility (Figure 4), apart from the window  $75.5 \text{ GeV} < m_X < 95.5 \text{ GeV}$ , where a small excess of data over the background prediction is observed. This excess, yielding to a global significance of  $1.43\sigma$ , corresponds to a  $m_Y$  value of about 3.7 TeV.

Post-fit  $p$ -values are computed for each  $m_Y$  bin in each  $m_X$  bin. Here, no significant deviations are observed. Also, given the absence of excess in background-only fit, upper limits at 95% of Confidence Level are determined from signal-plus-background fits on  $\sigma(pp \rightarrow Y \rightarrow XH \rightarrow q\bar{q}b\bar{b})$ .

## 2. – Graph Neural Network

Data with relational binding can be represented as nodes and connection between them and call this object as graph. Looking at this analysis, the strategy used is to portray reconstructed jets coming from the decay of heavy resonances using undirected graphs. Each node can be interpreted as a calorimeter topological cluster (topocluster) and the node features are the kinematical variables such the  $p_T$  fraction, the  $\eta$  and the  $\phi$ . The connections between nodes are based on spatial distance and two nodes are indeed

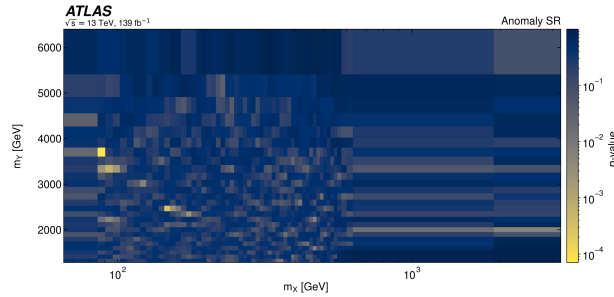


Fig. 4. – The distribution of observed  $p$ -values across all  $m_Y$  and  $m_X$  bins in the anomaly signal region, comparing data to the background estimation generated by a background-only fit, displayed in the two-dimensional  $(m_Y, m_X)$  grid. The lowest observed  $p$  corresponds to the bin with  $m_Y$  within  $[3608, 3805]$  GeV and  $m_X$  within  $[75.5, 95.5]$  GeV.

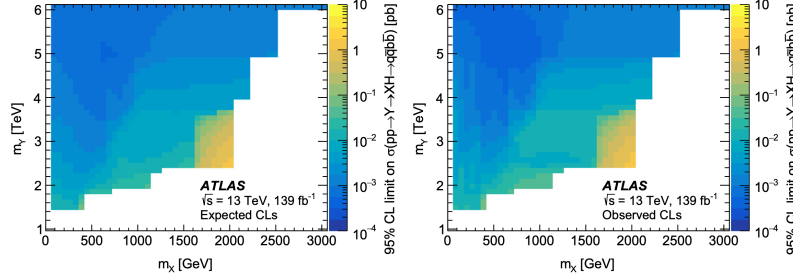


Fig. 5. – The expected (left) and observed (right) 95% CL limits on the cross-section  $\sigma(pp \rightarrow Y \rightarrow XH \rightarrow q\bar{q}b\bar{b})$  in  $pb$  in the two-dimensional space of  $m_Y$  versus  $m_X$ , obtained from a simultaneous fit of both merged and resolved two-prong signal regions with all statistical and systematic uncertainties. The observed limits range from  $0.341 fb$  for the signal point ( $m_Y = 5000$  GeV,  $m_X = 600$  GeV) to  $1.22$  pb for the signal point ( $m_Y = 2500$  GeV,  $m_X = 2000$  GeV).

connected if their relative distance  $\Delta R$  is less than a reference distance - e.g.  $\Delta R < 0.2$ , and each edge stores this information as a edge feature  $\frac{1}{\Delta R + \varepsilon}$ , where  $\varepsilon$  is used to avoid discontinuity.

A Graph Neural Network, or GNN, takes graphs with a variable number of nodes as input and can classify them with a given rule based on the structural and feature-based relationships between the nodes and edges between nodes. Each node receives information from its neighboring nodes through a mechanism known as message passing. This is a mechanism that allows nodes to aggregate and update their information based on the information received from adjacent nodes. Message passing has an iterative nature that allows GNNs to capture and propagate information across the entire graph, making it useful for tasks such as node classification, link prediction, and graph classification, which is the one we are looking at.

For benchmark results, the LHC Olympics 2020 [4] project is used. It aims to promote the development of ML models to identify jet events coming from a new resonance decaying fully hadronically among QCD background and presented a significant opportunity to test advanced methods in anomaly detection. The simulated data from this dataset were represented using graph structures: topoclusters considered as graph nodes and connections established between nodes with a distance criteria on the topoclusters - if  $\Delta R < 0.2$  an edge is established.

The simulated events used for this study consist in 1 million background QCD multi-jet production and 100 thousand of hypothetical new resonance  $W$  decaying into two vector boson  $X$  and  $Y$  with mass, respectively of 3.5 TeV, 500 GeV and 100 GeV.

The methodologies used are unsupervised learning using DeepSVDD (Deep Support Vector Data Description [6]) and performance evaluation using the area under the ROC curve for the Anomaly Score distribution. Even if unsupervised learning exhibits lower performance compared to supervised learning, it also offers an increased generalisation power, that is mandatory to promote model independence for the search of new physics.

During its training phase, the network work only with background data and optimises its parameters to lie within a hypersphere, as expressed in the DeepSVDD loss. When a signal event is presented at the network, this fall outside the hypersphere and is labelled as anomaly through the Anomaly Score (AS). The AS is computed at each epoch of the training process and its distribution is used as an indicator of the degree of anomaly of

that particular event.

The GNN used for this analysis is a Graph Isomorphism Network [7], with five layers of message passing. The approach was applied for both jet-level and event-level analysis, where the event-level results were obtained as an average of two jet.

The event-level anomaly score demonstrated strong discriminative power with an  $AUC = 84.3\%$ . Similarly, the jet-level anomaly score also showed significant effectiveness with an  $AUC = 77.9\%$ . For that case study, application of graph variables demonstrated a strong discriminative power.

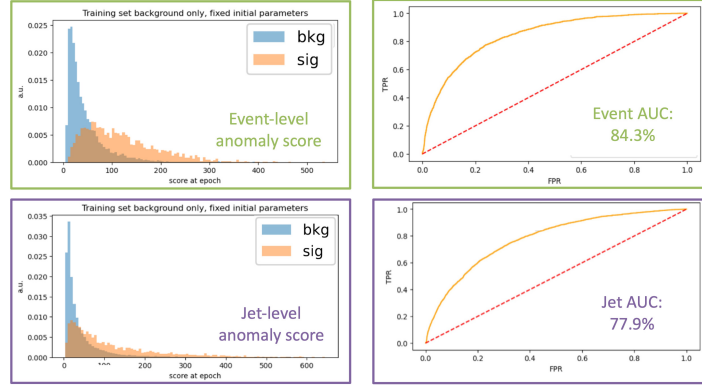


Fig. 6. – Summary of the LHC Olympics 2020 and the results of the anomaly detection using GNNs.

This unsupervised approach, as we can see from the ROC curve performances, lead to a good discriminant power that can be applied in anomaly detection technique. The next step is to use this paradigm on the Run-3 data collected by ATLAS.

## REFERENCES

- [1] ATLAS COLLABORATION, *Physical Review D*, **108** (2023) 052009
- [2] ATLAS COLLABORATION, *ATLAS  $b$ -jet identification performance and efficiency measurement with  $t\bar{t}$  events in  $pp$  collisions at  $\sqrt{s} = 13\text{ TeV}$*  *Eur. Phys. J.*, **C 79** (2019) 970
- [3] A. D’AVANZO, *Anomaly Detection search for new resonances decaying into a Higgs boson and a generic new particle  $X$  in hadronic final states using  $\sqrt{s} = 13\text{ TeV}$   $pp$  collisions with the ATLAS detector* *IL NUOVO CIMENTO*, **47 C** (2024) 113
- [4] KASIECZKA G. et al., *Welcome to the home of the LHC Olympics 2020!* <https://lhco2020.github.io/homepage/>, (2020)
- [5] G. RUSSO, *Searches for Anomalies in hadronic final states with GNNs in ATLAS* *IL NUOVO CIMENTO*, **47 C** (2024) 136
- [6] RUFF L. et al., *Deep One-Class Classification Proceedings of the 35th International Conference on Machine Learning*, **80** (2018) 4393-4402
- [7] XU K., et al., *How Powerful are Graph Neural Networks?* *arXiv*, **2019** (1810.00826v3)